ELSEVIER

Thermochimica Acta 366 (2001) 167–182

thermochimica acta

www.elsevier.com/locate/tca

State diagrams and sorption isotherms of bacterial suspensions and fermented medium

F. Fonseca, J.P. Obert, C. Béal, M. Marin*

Unité Mixte de Recherche de Génie et Microbiologie des Procédés Alimentaires (INRA–INA P-G), F-78850 Thiverval-Grignon, France

Received 3 May 2000; received in revised form 20 September 2000; accepted 20 September 2000

Abstract

Physical properties of lactic acid bacteria suspensions were determined by means of state diagrams and sorption isotherms. Differential scanning calorimetry (DSC) was used to establish the thermal transitions of concentrated ''fresh'' (before freeze-drying) and freeze-dried bacterial suspension equilibrated at different relative humidities. The bacterial cells and the re-suspending medium (fermented culture medium) were studied separately in order to determine each individual effect. No glass transition (T_g) was detected in thermal profiles of washed bacterial cells. Correspondingly, T_g curves were similar for fermented medium and bacterial suspension. Simple glass transitions (one heat capacity step) were observed at T_g in the case of low moisture samples. For samples containing more than 60.7% water, two steps remained in the glass transition region (T'_{g1} and T'_{g2}), even after annealing treatments. Water plasticising effect was well predicted by Gordon–Taylor equation. The invariant point (C'_g, T'_g), characteristic of maximally freeze-concentrated samples, was estimated from the intersection of the T_g curve and the melting curve T_m. A linear relationship was proposed to rapidly predict the T'_g region of complex aqueous solutions, from T'_g values of single solute aqueous solutions. Water sorption properties of fermented medium and bacterial suspension were determined at 25°C and described by the Guggenheim–Anderson–de Boer equation.

Keywords: Lactic acid bacteria; Glass transition; State diagrams; Water activity; Sorption isotherms

1. Introduction

Lactic acid bacteria (LAB) are widely used as starters for manufacturing cheeses, fermented milks, meats, vegetables and bread products. The preparation of starter cultures requires production and maintenance techniques that maximise storage stability, viability and activity of bacterial cells [1,2]. The conditioning of concentrated suspensions of LAB is currently performed by way of freeze-drying or freezing. The industrial choice depends on the nature of the bacteria and on economical and practical criteria.

Loss in bacteria viability and activity generally occurs during the different stages of starter manufacture and storage [3,2]. Changes in their physical state can also take place, since these biological materials are mainly composed of carbohydrates and proteins, which may be amorphous or partially amorphous [4]. In low moisture and frozen biological materials, molecular mobility and physicochemical properties are strongly related to water content and temperature.

* Corresponding author. Tel.: +33-1-30-815439; fax: +33-1-30-815597.
E-mail address: marin@grignon.inra.fr (M. Marin).

0040-6031/01/$ – see front matter
PII: S0040-6031(00)00725-5

Nomenclature

a_w	water activity
C	solids concentration (%, wet basis)
C'_g	solids concentration in the maximally freeze-concentrated phase (%, wet basis)
C_w	water content (%, wet basis)
C'_w	water content in the maximally freeze-concentrated phase (%, wet basis)
ΔC_p	change of specific heat capacity across the glass transition (J g^{-1} K^{-1})
D, K	GAB constants
ΔH_m	latent heat of ice melting (J g^{-1})
k	empirical parameter of Gordon–Taylor equation
m	moisture content (g g^{-1}, dry basis)
M	monolayer value (g g^{-1}, dry basis)
T_a	annealing temperature (°C)
T_g	glass transition temperature (°C)
T'_g	glass transition temperature of the maximally freeze-concentrated phase (°C)
T_m	melting temperature (°C)
X_w	mass fraction of water (g g^{-1}, dry basis)

The physical state of these natural polymers changes radically over the temperature range of glass transition — transformation from a solid glassy state to a viscous liquid with an increase of temperature or water content [4–7]. It has been assumed that amorphous materials, like food products, are more stable in their solid glassy state below the glass transition temperature (T_g), due to the high viscosity and the reduced molecular mobility of the solid glass, than in the rubbery state [8]. In order to better understand the changes that occur during processing and storage of LAB, their physical properties have to be determined.

State diagrams have been proposed to describe the different regions of the physical state of materials [9,10]. They show the relationship between material composition and temperature, and are usually established with measurements carried out by differential scanning calorimetry (DSC) [9–14]. In literature, state diagrams, associated to water sorption isotherms, have often been related to the dried product quality, and they have been used to explain the product stability during storage [15–17].

The aim of this study was therefore to determine the physical properties of lactic acid starters in their fermentation medium, by using the corresponding state diagrams and water sorption isotherms.

2. Materials and methods

2.1. Materials

The LAB *Lactobacillus bulgaricus* CFL1 was used as a model starter. It was provided by the Laboratoire de Génie et Microbiologie des Procédés Alimentaires (INRA, Thiverval-Grignon, France). Inoculum was stored at −70°C and thawed at 30°C for 15 min. The inoculation was carried out at a concentration of 10 g l^{-1}.

For starter production, the fermentation medium was composed of 56.6 g l^{-1} mild whey (BBA, Brenntag, Bonneuil sur Marne, France), heated at 110°C for 10 min and filtrated (0.2 μm). It was complemented with 20 g l^{-1} lactose (Prolabo, Paris, France), 5 g l^{-1} yeast extract (Labosi, Oulchy-Le-Chateau, France) and 1 ml l^{-1} antifoam (Rhodorsil 426R, Prolabo) and sterilised in the fermentor at 110°C for 20 min.

2.2. Production of lyophilised lactic acid bacteria

2.2.1. Starter production

Fermentation was performed at 42°C in a 2 l fermentor, stirred at 200 rpm. pH was controlled at 5.5, by adding 50.4 g l^{-1} NH_4OH solution, which was continuously weighted.

Cultures were stopped at the end of the exponential growth. This step was defined by the time at which NH_4OH consumption rate started to decrease. The cell suspension was rapidly cooled down to 15°C in the fermentor.

2.2.2. Concentration

Cells were harvested and concentrated by centrifugation (17 000*g*, 30 min, 4°C). With the cells, two kinds of samples were prepared for the study: bacterial suspension and washed bacterial cells. Half of the concentrated cells was re-suspended in the same weight of fermented medium to form the bacterial suspension. The other part of concentrated cells was washed three times successively with a sterile peptone water solution (1 g l^{-1}), in order to eliminate the

residual culture medium from the cells (washed bacterial cells).

2.2.3. Freeze-drying

Samples of washed cells and bacterial suspension, as well as samples of fermented medium were divided in aluminium pans (5 cm of diameter, 3.5 cm of height, without cover) in order to have a constant thickness of 1 cm in each pan (about 15 g of sample). A fixed thickness was necessary to have reproducible and homogeneous freezing rate as well as drying rate. The samples were frozen at −70°C in a cold air chamber. The freezing rate was around 1–2 cm h^{-1}.

Vacuum freeze-drying of samples was carried out in an SMH15 freeze-drier (Usifroid, Maurepas, France). In the freeze-dryer, the temperature of the sample, coming from the cold chamber, was first equilibrated with the cooling plate at −40°C. Then the drying process under vacuum is divided in two steps. During primary drying, which corresponds mainly to the sublimation of ice, the total pressure was kept at 50 Pa and the plate temperature was first raised from −40 to +10°C in 18 h, and afterwards, maintained at +10°C for 7 h. Preliminary studies in the laboratory have shown that in this range of pressure and temperature, the degradation of the samples are avoided (such as collapse). Slower drying kinetics are observed during a secondary step, corresponding to the desorption of the unfrozen water. A lower pressure (less than 15 Pa) and a higher temperature (60°C) are applied during the secondary drying in order to increase the mass transfer flux.

At the end of the process, the atmospheric pressure was recovered by using dry nitrogen gas. The dried samples were rapidly packed under vacuum, in aluminium bags. The freeze-dried samples were stored at −20°C before use in order to prevent, or at least to slow down, any reaction kinetics inside the product.

2.3. Conditioning at different relative humidities

Lyophilised samples of about 200 mg were equilibrated at 25°C under the following saturated salt solutions of constant water activities (a_w values are shown in parenthesis) [18]: CH_3COOK (0.23), $MgCl_2{\cdot}6H_2O$ (0.33), K_2CO_3 (0.44), $Mg(NO_3)_2{\cdot}6H_2O$ (0.53), KI (0.69), NaCl (0.75), KCl (0.84) and K_2SO_4 (0.98).

Equilibrium was assumed to be achieved when there was less than 1% variation in consecutive weighings, made at 48 h intervals.

2.4. Water content determination

Dry matter of the samples was determined after lyophilisation by maintaining samples at 60°C, less than 15 Pa, for 4 days. Water content of samples equilibrated at different relative humidities was determined gravimetrically from the weight gain of each sample.

2.5. Water activity measurement

Water activity of samples from sorption isotherms at 25°C was measured by an a_w meter FA-st/1 (Food Analysis Science and Technology, GBX Scientific Instruments, Romans sur Isère, France). Measurements were made with dynamic method and each result was the average value of at least 20 measurements, that were obtained after the stability was reached.

2.6. Differential scanning calorimetry

DSC was used to determine the glass transition and melting events of fermented medium, bacterial suspension and washed bacterial cells. Two kinds of samples were analysed: concentrated ''fresh'' samples, e.g. before freeze-drying, and samples that were freeze-dried and equilibrated to different relative humidities. DSC measurements were carried out using a differential scanning calorimeter Pyris 1 (Perkin-Elmer LLC, Norwalk, CT) equipped with a liquid nitrogen cooling accessory (CryoFill, Perkin-Elmer). Between 5 and 20 mg of each sample were placed in 50 μl Perkin-Elmer DSC hermetically sealed aluminium pans, and an empty pan was used as a reference.

Cooling and heating rates of 10°C min^{-1} were used throughout these studies. Blond and Simatos [5] reported that for concentrated sugar solutions, this scanning rate is low enough compared to relaxation rates. Samples were cooled to −120°C and scanned for the first time to 25°C to determine their thermal behaviour in the non-annealed state. They were cooled again to −120°C and heated to 60°C (fermented medium and bacterial suspension) or to 180°C

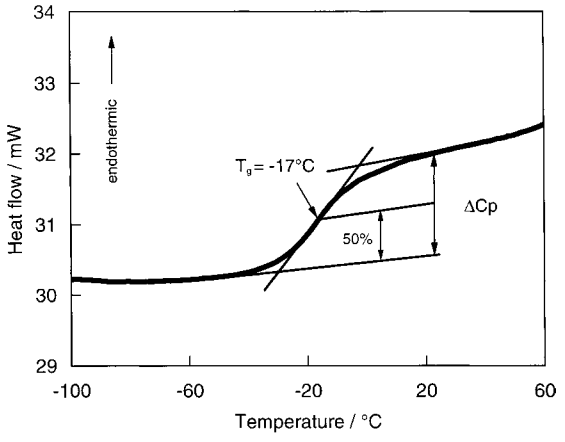

Fig. 1. DSC heating scan (10°C min^{-1}) of freeze-dried bacterial suspension, equilibrated at 53% relative humidity (25°C). ΔC_p: heat capacity change across the glass transition region (J g^{-1} K^{-1}); T_g: midpoint glass transition temperature (°C), corresponding to 50% of ΔC_p; sample weight: 11.3 mg.

(washed cells). Thermal properties were determined from the second heating scan in order to avoid possible time dependent changes in thermal behaviour [6].

As suggested by several authors [19,20], the temperature calibration was made using cyclohexane and mercury and mercury was used for the enthalpy calibration. In these calibration conditions, several parameters are obtained from the DSC scans corresponding to two main physical mechanisms. The ice melting can be characterised with the extrapolated peak onset temperature of the ice melting (T_m, in °C) [21] and with the latent heat of ice melting (ΔH_m, in J g^{-1}). As illustrated in Fig. 1, the glass transition can be represented by the midpoint temperatures (T_g, in °C) of the heat capacity steps associated to the glass transition with respect to the ASTM Standard Method E 1356-91,[1] and the relative variation of the heat capacity across the glass transition (ΔC_p, in J g^{-1} K^{-1}).

An isothermal annealing was applied to each sample showing an exothermic devitrification event, in order to obtain full ice crystallisation. In these cases, the first cooling was followed by a first heating up to the annealing temperature (T_a) (situated in the glass transition range) and the sample was cooled to −120°C again. The second heating scan was used to determine the characteristic glass transition temperatures (T_g, or T'_{g1} and T'_{g2} for samples at high water content), T_m and ΔH_m (by integration of the melting endotherm).

As shown in Tables 1 and 2, results are usually obtained from three or more DSC scans. In some exceptional cases, the results are based on two replicates, especially due to the difficulty to produce and to manipulate the bacteria samples.

2.7. Analytical methods

During the fermentation, the cell growth was estimated by absorbance measurements at 480 nm, after $\frac{1}{100}$ dilution. The concentrations of lactose, galactose, glucose and lactic acid in the culture medium were obtained using high-performance liquid chromatography (HPLC, Waters Associates, Milford, MA). After precipitating proteins with a trichloroacetic acid solution at a concentration of 240 g l^{-1}, samples were centrifuged for 30 min at 14 000*g* and filtered trough a membrane (pore diameter: 0.22 μm). A volume of 20 μl of a sample was injected automatically in a cation exchange column (Aminex HPX-87 H, 30 cm × 7.8 mm, BioRad, Richmond, CA). The column was maintained at 35°C and the mobile phase, a solution of H_2SO_4 at 0.005 M, was circulated at a 0.6 ml min^{-1} flow rate (Pump Waters 150, Millipore). At the outlet of the column, a refractometer (Waters 410, Millipore) was used as a detector and the results treatment was done with the Millenium software (Waters Version 3.0, Millipore). Propionic acid, at a concentration of 10 g l^{-1}, was used inside the sample as an internal reference.

3. Results and discussion

3.1. Differential scanning calorimetry profiles of biological samples

The thermal profiles of three kinds of samples were obtained by DSC: fermented medium (culture medium at the end of the fermentation), bacterial suspension (mixture of bacterial cells and fermented

[1] ASTM Standard test method for glass transition temperatures by differential scanning calorimetry or differential thermal analysis E 1356-91.

Table 1
Heat capacity step temperatures (T'_{g1} and T'_{g2}) of high relative humidity samples of concentrated "fresh" ($a_w > 0.98$) and freeze-dried fermented medium and bacterial suspension[a]

Water activity	Fermented medium[b]				Bacterial suspension[c]			
	n	Water content[d] (%)	T'_{g1} (°C)	T'_{g2} (°C)	n	Water content[d] (%)	T'_{g1} (°C)	T'_{g2} (°C)
0.98	5	60.7 (1.0)	−58.3 (0.8)	−43.0 (0.1)	2	66.3 (1.3) [65.0/67.6]	−58.3 (1.9) [−56.4/−60.2]	−40.2 (0.6) [−39.6/−40.7]
Concentrated ($a_w > 0.98$)	3	93.4 (0.1)	−57.6 (0.1)	−43.3 (0.2)	2	89.3 (0.1) [89.2/89.4]	−58.6 (0.5) [−58.1/−59.1]	−39.6 (0.4) [−39.2/−40.0]

[a] n: number of experimental data points; ( ): standard deviation; [/]: the two values obtained.
[b] Annealing temperature, $T_a = -45$°C.
[c] Annealing temperature, $T_a = -40$°C.
[d] Wet basis water content.

Table 2
Moisture content, midpoint glass transition temperatures (T_g) and melting temperatures (T_m) of concentrated ''fresh'' ($a_w > 0.98$) and freeze-dried fermented medium and bacterial suspensions, equilibrated at 25°C, at different water activities[a]

Water activity	Fermented medium				Bacterial suspension			
	n	Water content[b] (%)	T_g (°C)	T_m (°C)	n	Water content[b] (%)	T_g (°C)	T_m (°C)
0.23	7	3.6 (0.6)	11.1 (0.5)	NIM	4	2.7 (0.1)	22.1 (2.3)	NIM
0.33	4	5.5 (1.9)	−3.1 (2.9)	NIM	4	3.5 (0.1)	11.4 (0.9)	NIM
0.44	5	9.4 (1.5)	−22.0 (2.5)	NIM	5	6.2 (0.1)	−9.6 (1.1)	NIM
0.53	3	15.6 (0.1)	−42.0 (1.6)	NIM	2	7.6 (0.1) [7.7/7.5]	−17.5 (0.3) [−17.7/−17.2]	NIM
0.69	4	23.8 (1.5)	−68.2 (0.6)	NIM	4	18.8 (1.3)	−58.0 (3.2)	NIM
0.75	3	30.9 (0.1)	−79.0 (2.6)	−40.9 (0.2)	3	29.6 (1.9)	−72.5 (2.0)	−40.7 (0.1)
0.84	3	40.7 (0.2)	−92.4 (1.6)	−33.2 (0.4)	3	35.1 (0.1)	−83.4 (0.2)	−30.7 (0.7)
0.98	5	60.7 (1.0)	–	−12.3 (0.1)	2	66.3 (1.3) [65.0/67.6]	–	−10.1 (1.3) [−8.8/−11.3]
Concentrated ($a_w > 0.98$)	3	93.4 (0.1)	–	−2.4 (0.3)	2	89.3 (0.1) [89.2/89.4]	–	−3.1 (0.3) [−2.8/−3.4]

[a] n: number of experimental data points; –: not determined; NIM: no ice melting; ( ): standard deviation; [/]: the two values obtained.
[b] Wet basis water content.

medium) and washed bacterial cells (bacterial cells cleaned from culture medium).

3.1.1. Thermal behaviour of non-annealed samples

As a general result, significant changes in heat capacity, corresponding to second order glass transitions, were observed in the heating part of the DSC curves of freeze-dried fermented medium and bacterial suspension, equilibrated under different relative humidity atmospheres. The corresponding midpoint glass transition temperatures (T_g) were determined using the method given in Fig. 1.

Based on the enthalpy profile, three thermal behaviours were obtained, depending on the relative humidity (water activity) of each freeze-dried rehydrated sample of fermented medium and bacterial suspension:

- Samples equilibrated at less than 75% relative humidity showed no ice formation during freezing, and when rewarming, only one heat capacity step, corresponding to the glass transition, was observed (Fig. 1).
- Associated to a large peak of melting of the freezable water, two steps were identified in the heating scans of the samples equilibrated at 98% relative humidity (Fig. 2). The temperatures associated with these steps, T'_{g1} and T'_{g2}, characterised the glass transition [22]. Similar thermal profiles were observed in the case of concentrated "fresh" samples, e.g. before freeze-drying (water content: 93.4% for fermented medium and 89.3% for bacterial suspension).
- For samples equilibrated at a relative humidity of 75 and 84%, no water crystallisation was observed during cooling (Fig. 3a), indicating that vitrification was accomplished. However, an exothermic peak was observed during rewarming, between the glass transition and the melting endotherm (Fig. 3b). This process, generally called devitrification, corresponds to ice crystallisation [10]. Freezable water that had remained unfrozen due to hindered crystallisation during a fast cooling, crystallises during warming [23]. In this work, samples that presented a clear devitrification event, contained solute mass fractions between 0.59 and 0.70. These results are in accordance with MacKenzie's work [10], where he stated that devitrification is a feature associated, not only with rapid cooling but also with moderately concentrated solutions (solute mass fraction higher than 0.5).

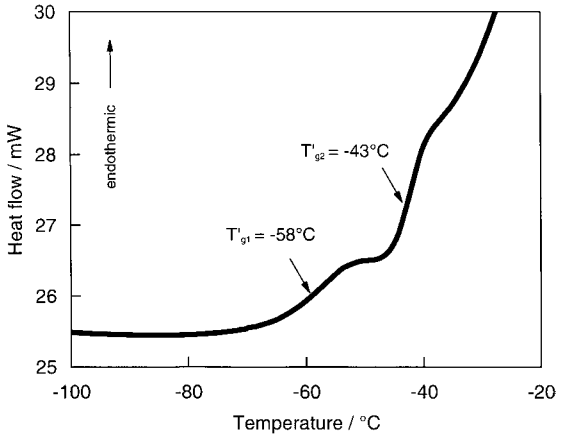

Fig. 2. DSC heating scan (10°C min^{-1}) of freeze-dried fermented medium, equilibrated at 98% relative humidity (25°C), after 8 h of annealing at −45°C. T'_{g1} and T'_{g2}: midpoint glass transition temperatures (°C); sample weight: 12.9 mg.

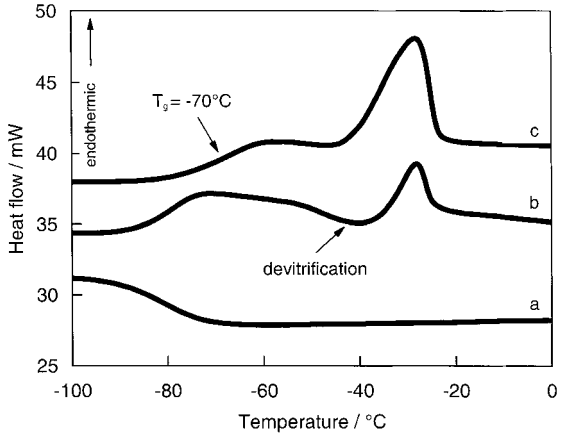

Fig. 3. DSC heating scan (10°C min^{-1}) of freeze-dried fermented medium, equilibrated at 75% relative humidity (25°C): (a) cooling scan; (b) first heating scan; (c) heating scan, after 8 h of annealing treatment at −45°C. T_g: midpoint glass transition temperature (°C); sample weight: 12.9 mg.

3.1.2. Thermal behaviour of annealed samples

According to Ablett et al. [12], after an optimum annealing procedure (isothermal treatment), leading to a maximal freeze-concentration of the solution, the devitrification event is eliminated and the two

transition steps coalesce. Optimum annealing conditions are obtained when the samples are maintained just above T'_g [12,20] or between T'_{g1} and T'_{g2} [19]. As in this work T'_g was not known in advance, an annealing temperature (T_a) between T'_{g1} and T'_{g2} and close to T'_{g2} was used ($T_a = -45°C$ for fermented medium and $T_a = -40°C$ for bacterial suspension).

The holding time associated to the annealing temperature is also critical. Blond and Simatos [20] have observed for a long annealing time in DSC thermograms of sucrose and dextran frozen solutions, an increase of enthalpy relaxation (called physical ageing) hiding the glass transition step. In this work, the duration of the annealing treatments was increased until values of T'_{g1} and T'_{g2} showed no further variation [14]. Isothermal annealing of 1 h eliminated the devitrification event and led to increase values of T'_{g1} and T'_{g2} (Fig. 3c). Eight hours of annealing did not further modify the thermal profiles.

From Fig. 2, two transitions are still evident after annealing treatments of 8 h, for freeze-dried samples of fermented medium equilibrated at 98% relative humidity. After the same annealing treatment, similar profile, with two steps, were obtained with freeze-dried samples of bacterial suspension equilibrated at 98% relative humidity as well as samples of concentrated "fresh" fermented medium. According to Ablett et al. [24], the two steps could be due to an imperfect annealing and the finite scan rates applied to samples during experiments. This complex feature, observed for biological products, could also be the result of the superposition of the glass transition with other thermal events, like small ice dissolution in the maximally freeze concentrated solution [25], onset of ice melting [6], enthalpy relaxation process [11], or real-time softening process [26]. The persistence of this double transition, even after long annealing treatments, has already been reported for sugar solutions [5,26], glass forming salts [27] and organic acids [28]. Furthermore, it remains a subject of debate whether T'_g value corresponds to the onset of T'_{g1} [19], rather than to the midpoint of T'_{g1} [12], or to the midpoint of T'_{g2} [29] or if it must be considered as a temperature range [22]. In this work, both midpoint temperatures, T'_{g1} and T'_{g2}, were kept for characterisation of the glass transition presented by samples at high water content.

From Table 1, T'_{g2} value was 3°C higher when cells were added to fermented medium than in their absence, while T'_{g1} was not significantly different. The heat capacity step taking place at T'_{g2} seems to be dependent on the presence of bacteria in the fermented medium.

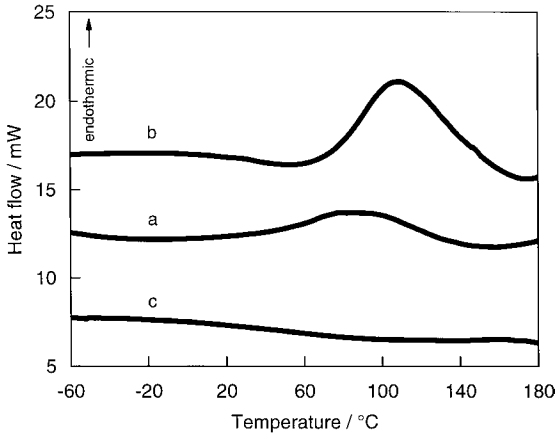

Fig. 4. DSC heating scan (10°C min^{-1}) of freeze-dried and rehydrated washed cells of two water contents: (a) 16% water content wet basis, sample weight, 5.0 mg; (b) 9% water content wet basis, sample weight, 9.2 mg; (c) immediate re-scan of sample at 9% water content wet basis.

3.1.3. Thermal behaviour of washed bacterial cells

In order to study the possible effect of bacteria on the thermal behaviour of biological media, washed bacterial cells were freeze-dried and rehydrated to different water contents. From Fig. 4, whatever the water content of the sample (curves (a) and (b)), glass transition were not identified by DSC in the temperature range studied (from −60 to +180°C). For multicomponent systems like cell wall material from apple which is also a complex biological material, Aguilera et al. [30] has suggested that DSC techniques could be insensitive to glass transition when changes in heat capacity are small and if many transitions occur in the same temperature range. However, no maximum value were observed in the derivative curve of the heat flux, and non-significant change of heat capacity (higher than 0.03 J g^{-1} K^{-1}) was determined all along the curves (a) and (b) from Fig. 4.

Moreover, an endothermic event starting at 40°C was observed during heating from −80 to 180°C (curves (a) and (b) in Fig. 4). Peak temperatures were in the range 70–110°C, and endotherm size increased with water content (from curve (a) to curve (b) in

Fig. 4). But, no peak at all was observed after an immediate re-scan indicating the irreversible character of this phenomenon (curve (c) in Fig. 4). Similar endothermic events have been reported for low moisture food products [30], polysaccharides [31,32], proteins [33] and bacterial spores [34]. Water evaporation [30,33], H-bonding rearrangement polysaccharides [31], carbohydrate–water [32] and protein–water [33] interactions and thermal denaturation processes [35] have been invoked to explain this endotherm.

As a conclusion, it can be pointed out that freeze-dried samples of the washed bacterial cells studied did not show a glass transition step with DSC method.

3.1.4. Glass transitions and melting temperatures

The T_g and T_m values obtained for the samples of fermented medium and bacterial suspension, are given in Table 2, as a function of the water content in the medium. T_g values were determined only for samples equilibrated under water activities lower than 0.98. Referring to the same water content, whatever the medium, similar T_g and T_m values were obtained (i.e. water content $= 3.6-3.5\%$, $T_g = 11.1-11.4°C$; water content $= 30.9-29.6\%$, $T_m = -40.9-40.7°C$). Therefore, it confirms that the difference of the composition between fermented medium and bacterial suspension, due to the presence of the bacteria cells in the last case, do not modify neither the glass transition nor the melting temperature observed for the whole medium.

Moreover, for each medium, T_g decreased and T_m increased with increasing moisture content, due to the well-known plasticising effect of water in the biological medium. Referring to Table 2, T'_{g2} was higher for bacterial suspension than for fermented medium (at fixed water activity), which can be now clearly related to the differences in water content (lower water content for bacterial suspension).

The effect of water on T_m could also have been expected on the basis of ideal solution behaviour: the higher the solute concentrations, the higher the observed freezing point depression [36].

3.2. State diagrams of biological samples

3.2.1. Prediction of glass transition temperatures

The Gordon–Taylor equation was originally developed to predict the glass transition temperature (T_g) of binary blends of miscible polymers [37]. It has also been used to represent the T_g depression of various amorphous sugars [38] and food materials [17], as a result of water plasticisation. The Gordon–Taylor equation was used to model the T_g curve of both freeze-dried fermented medium and bacterial suspension at different water contents, in order to establish the corresponding state diagrams, with:

$$T_{gm} = \frac{X_w T_{gw} + k(1 - X_w) T_{gs}}{X_w + k(1 - X_w)} \quad (1)$$

where T_{gm}, T_{gs}, and T_{gw}, are the glass transition temperatures (K) of the mixture, of the solids and of the water, respectively, X_w is the mass fraction of water, and k is a constant. The glass transition temperature of pure water was taken as $T_{gw} = -135°C$ [39]. Using the assumption proposed by Couchman and Karasz [40], that the heat capacity increments of the components at the glass transition are temperature independent, the constant k is equivalent to the ratio of the change of the component heat capacity ($k = \Delta C_{pw}/\Delta C_{ps}$ — water/solids). However, poor correlation have been reported by Roos et al. [6] and Blond et al. [22] between experimental and calculated T_g values of carbohydrate solutions, using ΔC_p values of solids and of water (ΔC_{pw} varying from 0.11 [41] to 1.94 J g^{-1} K^{-1} [42]). Therefore, k values were empirically determined as an adjustable parameter of Eq. (1).

As the T_{gs} value of completely dried samples are difficult to achieve experimentally, Eq. (1) was rearranged for the simultaneous evaluation of T_{gs} and k, by least-square regression:

$$T_{gm} = T_{gs} + \frac{kX_w}{1 - X_w}(T_{gw} - T_{gm}) \quad (2)$$

Each experimental data series respectively for fermented medium and for bacterial suspension were separately fitted to the Eq. (2) and the curves (continuous line for bacterial suspension and dotted line for fermented medium) are given in Fig. 5. The resulting parameters k and T_{gs} for each curve are given in Table 3. The curves for fermented medium and for bacterial suspension superimpose. The data can be considered as similar for fermented medium whether the bacterial cells were present or not, as a function of the water content. Again, it confirms that the effect of bacteria on T_g value of a whole biological

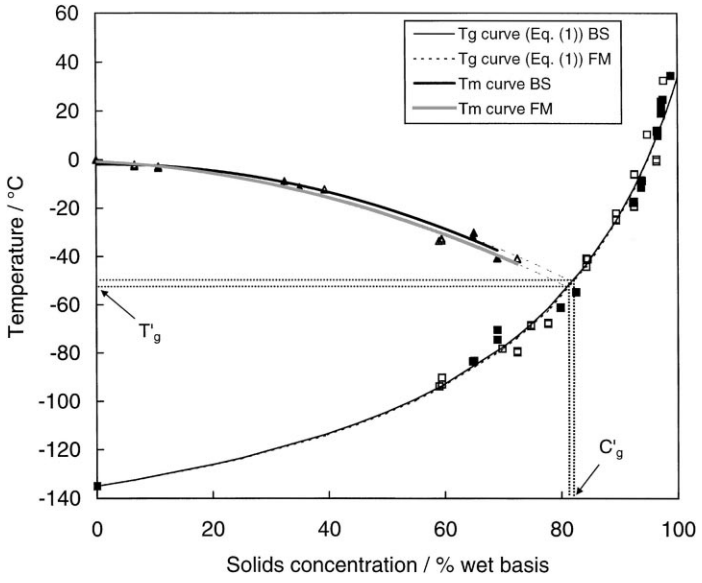

Fig. 5. State diagrams of bacterial suspension (BS, closed symbols) and fermented medium (FM, open symbols). The location of the glass transition temperature of the maximally freeze-concentrated phase (T'_g) and the concentration of the solids in this maximally freeze-concentrated matrix (C'_g), determined as the intersection of T_m and T_g curves, are indicated with arrows: $(C'_g, T'_g) = (81.9\%, -50.4°C)$ for bacterial suspensions and $(C'_g, T'_g) = (81.3\%, -52.9°C)$ for fermented medium.

medium is only related to the moisture content variation of this medium. Consequently, the T_g curve of bacterial suspension could be determined by thermal properties of the re-suspending medium.

Based on the composition of the fermented medium (Table 3), the whole prediction of the complex medium T_g curve is not possible, as no state diagram has been reported for ammonium lactate. This organic salt is not commercially available and due to components high water content, it was not possible to prepare it at a concentration higher than 33% (wet basis). Nevertheless, k and T_{gs} literature values for lactose, galactose and glucose [38] were collected in Table 3. Lactose is at higher concentration in the fermented

Table 3
Composition of the fermented medium, glass transition temperatures of dry samples (T_{gs}) and estimated k values of Gordon–Taylor equation[a]

Sample	Fermented medium composition (%)[b]	T_{gs} (°C)	k	r^2	Refs.
Lactose	2.95 ± 0.05	101[c]	6.56		[38]
Galactose	1.26 ± 0.04	30[c]/38[d]	4.49		[38]
Ammonium lactate	1.35 ± 0.01	–	–		–
Glucose	0.18 ± 0.01	31[c]/36[d]	4.52		[38]
Fermented medium[e]		33.7[d] (3.3)	4.6 (0.2)	0.958	This work
Bacterial suspension[e]		33.6[d] (3.0)	4.5 (0.4)	0.953	This work

[a] ( ): standard deviation; r^2: coefficient of determination to Eq. (2); – no reference available.
[b] Determined by HPLC.
[c] Onset temperature.
[d] Midpoint temperature.
[e] Eq. (2) was applied to each set of experiments: to the fermented medium at variable water content and to the bacterial suspensions at variable water content.

medium than glucose and galactose, but the parameters k and T_{gs} of the complex medium studied are rather closer to those of galactose and glucose than to lactose ones. It could be due to the additional effect of ammonium lactate. This component was observed to decrease the value of T'_g of frozen biological medium [43].

3.2.2. Prediction of the melting temperature

Raoult's law allows the prediction of freezing temperature of an ideal medium from a_w data. As expected, our results showed a poor correlation between predicted and experimental T_m values, especially for samples of high solids content: a ΔT_m ($T_{m\,predicted} - T_{m\,measured}$) value of about 15°C was obtained for 59.3% solids concentration (C, wet basis). Moreover, the non-ideal character of samples analysed was also confirmed by the poor fitting of Chen [36] equation to experimental T_m data. This equation, derived on the basis of a modified Raoult's law, incorporates semi-empirical modifications to consider this non-ideal behaviour, but it did not offer accurate T_m estimations in the range studied ($\Delta T_m = 12$°C; $C = 59.3\%$).

Consequently, experimental values of onset melting of fermented medium and bacterial suspension were fitted to a second order empirical equation based on the results of Chang and Tao [44] for sugar containing solutions. In this work, the following relationships were obtained:

$$T_m = -0.0065C^2 - 0.1133C - 0.7042,$$
$$r^2 = 0.981 \text{ for fermented medium}$$
$$T_m = -0.0071C^2 - 0.0148C - 1.5703,$$
$$r^2 = 0.984 \text{ for bacterial suspension}$$

where T_m is the melting temperature in (°C), C the solute concentration (% solids wet basis).

It was not possible to obtain T_m data above 70% solids concentration (Table 2) due to the kinetic restraints of highly concentrated solutions.

3.2.3. Properties at maximum freeze concentration (T'_g, C'_g)

The pioneering work of Levine and Slade [4] has highlighted the technological significance of the glass transition temperature of the maximally freeze-concentrated phase (T'_g). The concentration of the solids in this maximally freeze-concentrated matrix (C'_g, % solids wet basis), is independent of initial solute concentration.

In this study, three different approaches have been used to determine the (T'_g, C'_g) invariant point:

- A first method, proposed by Levine and Slade [29], calculates the C'_g concentration from the area under the ice melting endotherm. These authors designated the second transition in the DSC curve (T_{g2}) as the glass transition of the maximally freeze-concentrated solution, T'_g. However, several authors have largely criticised the assignment of T_{g2} to T'_g [12,19,22,26], associating T'_g to T_{g1} rather than T_{g2}.
- In a second method, firstly proposed by Simatos et al. [45] and largely used by other authors [6,14,38], the unfreezable water content ($C'_w = 100 - C'_g$) has been determined at first, from the linear relationship between the latent heat of ice melting (ΔH_m, in J g^{-1}) of annealed samples and moisture content (C_w, in % wet basis). C'_g is calculated by extrapolation to $\Delta H_m = 0$ and corresponds to the T'_g value, which can be evaluated using Gordon–Taylor equation (Eq. (1)).
- A third method, proposed by Franks [46], is based on the extrapolation of the T_m curve until it meets the T_g curve (Fig. 5). Although the accuracy of this determination has been contested [22], it allows a rather good estimation of T'_g and C'_g [12,22].

Table 4 shows the T'_g and C'_g values obtained with the three methods for the fermented medium and the bacterial suspension, in concentrated "fresh" (first method) and freeze-dried (second and third methods) forms.

The concentrations for the maximally freeze-concentrated solution, C'_g, were the lowest when calculated by the first method. This result was expected, since Hatley et al. [47] have already pointed out the inaccuracy of C'_g determination from the melting endotherm. The integration used to determine the ice fraction may be subject to errors that lead to the under-estimation of C'_g. These errors arise from the DSC profile that generally contains not only the heat capacity of ice melting but also the heat of dilution [47] and stress relaxation contributions [48]. The temperature dependence of the latent heat of fusion,

Table 4
Glass transition temperature (T'_g) and solute concentration (C'_g) of the maximally freeze-concentrated amorphous matrix, calculated by different methods

Method	Fermented medium		Bacterial suspension	
	C'_g (%)	T'_g (°C)	C'_g (%)	T'_g (°C)
First [29]	64.8	(−57.6/−43.3)[a]	75.3	(−58.6/−39.6)[a]
Second [45]	75.1	−68.1	77.3	−62.4
Third [46]	81.3	−52.9	81.9	−50.4

[a] (T'_{g1}/T'_{g2}): experimental values corresponding to concentrated samples submitted to an 8 h annealing treatment (fermented medium at −45°C; bacterial suspension at −40°C).

not currently considered for area calculation, is another source of error [47].

With the second method, the latent heat of melting was found to be a linear function of the water content, for fermented medium ($\Delta H_m = 3.99C_w - 99.3$, $r^2 = 0.994$) and bacterial suspension ($\Delta H_m = 3.91C_w - 88.8$, $r^2 = 0.972$). This method provided higher C'_g values than the first one (Table 4), but they were still lower than values reported by Roos [38] for galactose ($C'_g = 80.5\%$) and lactose ($C'_g = 81.3\%$).

The C'_g values obtained from the intersection of T_m and T_g curves, using the third method, were the highest ones, and they were similar to galactose and lactose values from Roos [38]. T'_g values obtained by this method were ranged between the T'_{g1} and T'_{g2} values presented for the annealed samples at high water content.

We have to keep in mind that the glass transition event takes place in a temperature range [20], due to the complex composition of the medium studied. Nevertheless, the intersection point seems to give a good estimation of the invariant T'_g value that can be used for comparing samples of different compositions. The average value of T'_g for fermented medium and bacterial suspension was close and equal to −51.7°C (±1.3°C).

3.2.4. Prediction of T'_g of aqueous solutions

In order to have a rapid estimation of T'_g temperature range of the complex biological medium studied, without determining the whole state diagram, an alternative approach can be proposed. DSC studies have already been performed to characterise model solutions closed to the biological media used for the LAB production [43]. It has been observed that model aqueous mixture of lactose, galactose and lactic acid present two step glass transitions, and that these T'_g belong to the range of the T'_g values observed for each single component aqueous solution [43]. In this work, we propose a simple linear relationship (Eq. (3)) to predict the T'_g values of the fermented medium (T'_{g1m} and T'_{g2m}), from T'_g and concentration values of binary aqueous solutions:

$$T'_{gm} = \frac{\sum T'_{gi} C_i}{\sum C_i} \quad (3)$$

where T'_{gi} and C_i are, respectively, the T'_g temperature (°C) and the solute concentration in water (% solids, wet basis) of each component i: lactose, galactose, ammonium lactate and glucose (Table 3). The T'_{gi} values of lactose, galactose and glucose were taken as the T'_g and T'_m midpoint values reported by Roos [38], for predicting T'_{g1m} and T'_{g2m}, respectively. In the case of ammonium lactate, the T'_{gi} values used for calculation were those reported by Fonseca et al. [43], obtained after 8 h of annealing treatment at −70°C, $T'_{g1} = -81.0$°C and $T'_{g2} = -61.7$°C.

From Eq. (3), the T'_{g1m} and T'_{g2m} values of the fermented medium were −52.5±0.1°C and −42.9± 0.1°C, respectively. There was no difference between the estimation and the measured value of T'_{g2} (Table 1). However, for T'_{g1}, the estimation was 5°C higher than the experimental value. This difference can be ascribed to small quantities of other components that are present in the fermented medium, i.e. soluble proteins and salts. An annealing treatment insufficient to obtain a maximally freeze-concentrated solution can also explain this discrepancy.

These results pointed out that T'_g values of the fermented media were strongly related to T'_g values of binary aqueous solutions, depending linearly on the

solute concentration. As already mentioned for the T_g values, the bacterial cell components do not specifically affect the glass transition behaviour (T'_g) of the whole fermented medium at high water content. Then, Eq. (3) gave a reasonable estimation of the T'_g values of the complex biological medium studied based on the main solute concentration except the bacteria cells. It can be used, for instance, to predict the effect on T'_g values of the addition to the "conditioning" medium (e.g. the fermented medium in this case), of another solute like a cryoprotectant.

3.3. Water sorption isotherms of biological samples

The biological materials studied showed substantial differences in water sorption properties: 3 weeks were necessary for the equilibration of fermented medium and 1–2 months for bacterial suspension at various a_w values.

Water sorption isotherms show relationships between a_w and water content at a constant temperature. Modelling studies of sorption properties are particularly important in predicting shelf life of low and intermediate-moisture foods [13,16,49]. The Brunauer–Emmet–Teller (BET) [50] and Guggenheim–Anderson–de Boer (GAB) [13] equations are well-known models that provide the monolayer value (M, in g g^{-1} dry basis), often considered as the optimal water content for stability of low-moisture foods [49].

The experimental data of fermented medium and bacterial suspension were fitted to the GAB model (Eq. (4)) due to its applicability over a wider range than the BET model [13,16,17]:

$$m = \frac{MDKa_w}{(1 - Ka_w)(1 - Ka_w + DKa_w)} \quad (4)$$

where m is the water content (g g^{-1}, dry basis), M the moisture content at fully occupied active sorption sites with one molecule of water M (g g^{-1}, dry basis), D and K are adjustable parameters.

Eq. (4) was transformed to the form of a second order polynomial [13], as follows:

$$\frac{a_w}{m} = \alpha a_w^2 + \beta a_w + \gamma \quad (5)$$

where α, β and γ are constants that were obtained by plotting a_w against a_w/m. The constants K, D and the monolayer value (M) were calculated from Eqs. (6)–(8), respectively:

$$M^2 = \frac{1}{\beta^2 - 4\alpha\gamma} \quad (6)$$

$$K = \frac{(1/M) - \beta}{2\gamma} \quad (7)$$

$$D = \frac{1}{MK\gamma} \quad (8)$$

Table 5 shows GAB parameters for both fermented medium and bacterial suspension, as well as the correlation coefficients. According to literature data on complex medium [13], the GAB isotherm showed a good agreement with the experimental adsorption data for the a_w range studied. The monolayer values, M, were of the same order as those obtained for different fruits [17], and for milk powders [13,16] which contain similar sugars (mono and disaccharide). M value for fermented medium was higher in the absence (0.16) than in the presence of bacteria (0.11). The monolayer value was previously proposed to be the critical water content below which dehydrated foods are stable [13]. In this sense, bacterial suspension would be stable at a water content 5% lower than fermented medium. However, Karmas et al. [51] indicated that stability and the rates of degrading reactions of biological materials are related to the mobility above the glass transition temperature, rather than to the monolayer value. Thus, it should be better

Table 5
Monolayer value (M) and constants K and D for the GAB isotherm[a]

Material	a_w range[b]	n	M (g g^{-1} dry basis)	K	D	r^2
Fermented medium	0.23–0.98	23	0.158	0.998	0.724	0.881
Bacterial suspension	0.23–0.98	25	0.106	1.005	0.682	0.843

[a] n: number of experimental data points; r^2: coefficient of determination for the quadratic regression, $a_w/m = \alpha a_w^2 + \beta a_w + \gamma$.
[b] Water activity range of experimental sorption data.

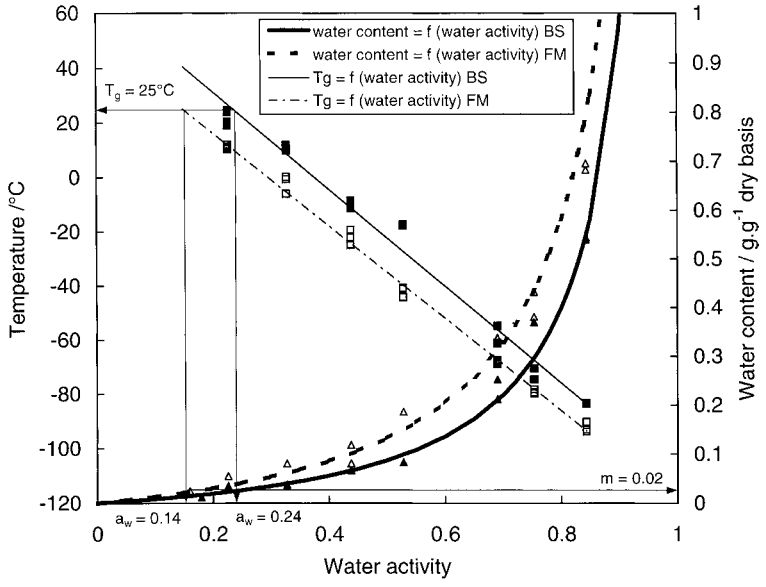

Fig. 6. Relationships between glass transition temperature (T_g), water activity (a_w) and the water content (m) for bacterial suspension (BS, closed symbols) and fermented medium (FM, open symbols). Arrows indicate the location of critical T_g, a_w and m values at 25°C.

to consider the critical water content and critical water activity values, as those that depress T_g to storage temperature. The relationship between a_w and T_g is sigmoidal over the whole a_w range [16]. Nevertheless, Roos [52] established a linear relationship that generally applies over the a_w range of 0.1–0.8. In this work, the samples showed linear relationships over the a_w range of 0.23–0.84 with

$$T_g = -171.5a_w + 51.0,$$

$$r^2 = 0.996 \text{ for fermented medium}$$

$$T_g = -179.1a_w + 67.5,$$

$$r^2 = 0.985 \text{ for bacterial suspension}$$

Storage stability of biological materials can be predicted by a single plot, presenting the relationships between glass transition temperature, water content and relative humidity at equilibrium [38] (Fig. 6). Referring to the critical T_g of 25°C for storage at ambient temperature [15], fermented medium showed a lower critical a_w (0.14) than bacterial suspension studied (0.24). Nevertheless, both materials presented similar critical moisture content (0.02 g g^{-1} dry basis). In both cases the monolayer values were higher than the critical water contents. This agrees with the results of Jouppila and Roos [15,16], who reported critical water contents at 24°C for stability of lactose and milk powders, above the monolayer value.

The results indicated that, at a storage temperature of 25°C, freeze-dried bacteria re-suspended in the fermented medium studied should be stored at relative humidity lower than 24%. Knowing that industrial practice do not assure to apply a low humidity value respect to the medium composition, the freeze-dried bacteria are usually commercially available at 4°C. The sorption isotherm and the state diagram can also be related to biological activity measurements of bacteria to establish, for a given starter, the maximal storage temperature for stability and shelf life requirements.

4. Conclusions

Fermented medium and bacterial suspension of LAB were analysed with DSC equipment. In the case of samples equilibrated under high relative humidities, annealing was necessary to eliminate devitrification and to obtain reproducible glass transition temperatures.

The cell bacteria did not present a characteristic T_g detectable by DSC in the temperature range −120 to

+180°C. No specific effect of bacterial components (cells) in the fermented medium on the DSC profile was observed, except the resulting effect of the increase of the dry matter content. As a consequence, the nature of the compounds used for the bacteria ''conditioning'' medium (e.g. the fermented medium in this case) determines the glass transition of the final mixture, which is a function of the water content based on the well-known plasticising effect. Nevertheless, the monolayer level of water of bacterial suspension differs from the fermented medium ones, leading to different water activities for the same water content.

The applicability of previously known models, like Gordon–Taylor equation for glass transition and GAB equation for water sorption, to the complex biological media studied, was verified in the experimental range studied. Using the state diagrams and sorption isotherms, that characterised these media, two regions were defined: one of low mobility (glassy) and the other of increased mobility (rubbery). The critical water content and relative humidity values for physical freeze-dried bacteria stability were established as a function of the storage temperature.

Moreover, a simple linear relationship was proposed for predicting the T'_g temperature region of complex aqueous solutions from the T'_g and the concentration values of single solute aqueous solutions.

In the future, the state diagrams and the sorption isotherms of lactic acid starters, associated to measurements of bacterial biological activity, could be a useful approach for the formulation of the conditioning medium, in order to optimise bacteria quality and stability during processing and storage.

Acknowledgements

The authors acknowledge the support of Eiffel programme (CIES, France).

References

[1] J. Stadhouders, Neth. Milk Dairy J. 40 (1986) 115.
[2] F. Fonseca, C. Béal, G. Corrieu, J. Dairy Res. 67 (2000) 83.
[3] C. Béal, G. Corrieu, Lebensm. Wiss. u. Technol. 27 (1994) 86.
[4] H. Levine, L. Slade, Cryo-Lett. 9 (1988) 21.
[5] G. Blond, D. Simatos, Thermochim. Acta 175 (1991) 239.
[6] Y. Roos, M. Karel, J. Food Sci. 56 (1991) 1676.
[7] F. Franks, Pure Appl. Chem. 65 (1993) 2527.
[8] H. Levine, L. Slade, in: V.R. Harwalkar, C.Y. Ma (Eds.), Thermal Analysis of Foods, Elsevier Applied Science, London, 1990, p. 221.
[9] F. Franks, M.H. Asquith, C.C. Hammond, H.B. Skaer, P. Echlin, J. Microsc. 110 (1977) 223.
[10] A.P. MacKenzie, J. Res. Nat. Bur. Stand. (US) 278 (1977) 167.
[11] G. Blond, Cryo-Lett. 10 (1989) 299.
[12] S. Ablett, M.J. Izzard, P.J. Lillford, J. Chem. Soc., Faraday Trans. 88 (1992) 789.
[13] Y.H. Roos, J. Food Process. Preserv. 16 (1993) 433.
[14] M.M. Sa, A.M. Sereno, Thermochim. Acta 246 (1994) 285.
[15] K. Jouppila, Y.H. Roos, J. Dairy Sci. 77 (1994) 2907.
[16] K. Jouppila, Y.H. Roos, J. Dairy Sci. 77 (1994) 1798.
[17] M.M. Sa, A.M. Figueiredo, A.M. Sereno, Thermochim. Acta 329 (1999) 31.
[18] L. Greenspan, J. Res. Nat. Bur. Stand. (US) 81A (1977) 89.
[19] Y. Roos, M. Karel, Int. J. Food Sci. Technol. 26 (1991) 553.
[20] G. Blond, D. Simatos, Food Hydrocoll. 12 (1998) 133.
[21] G.W.H. Höne, H.K. Cammenga, W. Eysel, E. Gmelin, W. Hemminger, Thermochim. Acta 160 (1990) 1.
[22] G. Blond, D. Simatos, M. Catté, C.G. Dussap, J.B. Gros, Carbohydr. Res. 298 (1997) 139.
[23] D.R. MacFarlane, Cryobiology 23 (1986) 230.
[24] S. Ablett, A.H. Clark, M.J. Izzard, P.J. Lillford, J. Chem. Soc., Faraday Trans. 88 (1992) 795.
[25] B. Luyet, D. Rasmussen, Biodynamica 10 (1968) 167.
[26] E.Y. Shalaev, F. Franks, J. Chem. Soc., Faraday Trans. 91 (1995) 1511.
[27] B.S. Chang, C.S. Randall, Cryobiology 29 (1992) 632.
[28] A.B. Andersen, L.H. Skibsted, Lebensm. Wiss. u. Technol. 31 (1998) 69.
[29] H. Levine, L. Slade, J. Chem. Soc., Faraday Trans. 84 (1988) 2619.
[30] J.M. Aguilera, T.R. Cuadros, J.M. del Valle, Carbohydr. Polym. 37 (1998) 79.
[31] M.J. Gidley, D. Cooke, S. Ward-Smith, in: J.M.V. Blanshard, P.J. Lillford (Eds.), The Glassy State in Foods, Nottingham University Press, Nottingham, UK, 1993, p. 303.
[32] I.A.M. Appelqvist, D. Cooke, M.J. Gidley, S.J. Lane, Carbohydr. Polym. 20 (1993) 291.
[33] V. Samouillan, J. Dandurand-Lods, A. Lamure, E. Maurel, C. Lacabanne, G. Gerosa, A. Venturini, D. Casarotto, L. Gherardini, M. Spina, J. Biomed. Mater. Res. 46 (1999) 531.
[34] S. Ablett, A.H. Darke, P.J. Lillford, D.R. Martin, Int. J. Food Sci. Technol. 34 (1999) 59.
[35] Z.Y. Ju, N. Hettiarachchy, A. Kilara, J. Dairy Sci. 82 (1999) 1882.
[36] C.S. Chen, J. Food Sci. 52 (1987) 433.
[37] M. Gordon, J.S. Taylor, J. Appl. Chem. 2 (1952) 493.
[38] Y. Roos, Carbohydr. Res. 238 (1993) 39.
[39] G.P. Johari, A. Hallbrucker, E. Mayer, Nature 330 (1987) 552.
[40] P.R. Couchman, F.E. Karasz, Macromolecule 11 (1978) 117.
[41] A. Hallbrucker, E. Mayer, G.P. Johari, J. Phys. Chem. 93 (1989) 7751.

[42] M. Sugisaki, H. Suga, S. Seki, Bull. Chem. Soc. Jpn. 41 (1968) 2591.
[43] F. Fonseca, M. Marin, C. Béal, in: Tec, Doc (Eds.), Proceedings of the Agoral'99, Nantes, France, 1999, p. 283.
[44] H.D. Chang, L.C. Tao, J. Food Sci. 46 (1981) 1493.
[45] D. Simatos, M. Faure, E. Bonjour, M. Couach, Cryobiology 12 (1975) 202.
[46] F. Franks, in: D. Simatos, J.L. Multon (Eds.), Properties of Water in Foods, Martinus Nijhoff, Dordrecht, 1985, p. 497.
[47] R.H.M. Hatley, C. van den Berg, F. Franks, Cryo-Lett. 12 (1991) 113.
[48] R.H.M. Hatley, A. Mant, Int. J. Biol. Macromol. 15 (1993) 227.
[49] T. Labuza, Food Technol. 34 (1980) 36.
[50] S. Brunauer, P.H. Emmet, E. Teller, J. Am. Chem. Soc. 60 (1938) 309.
[51] R. Karmas, M.P. Buera, M. Karel, J. Agric. Food Chem. 40 (1992) 873.
[52] Y. Roos, J. Food Sci. 52 (1987) 146.